Real-time Performance of the Virtual Seismologist Earthquake Early Warning Algorithm in Southern California

Georgia Cua,[1] Michael Fischer,[1] Thomas Heaton,[2] and Stefan Wiemer[1]

INTRODUCTION

The Virtual Seismologist (VS) method is a Bayesian approach to regional network-based earthquake early warning (EEW) that estimates earthquake magnitude, location, and the distribution of peak ground motion using observed ground motion amplitudes, predefined prior information, and appropriate attenuation relationships (Cua 2005; Cua and Heaton 2007). The application of Bayes's theorem in earthquake early warning (Cua 2005) states that the most probable source estimate at any given time is a combination of contributions from prior information (possibilities include network topology or station health status, regional hazard maps, earthquake forecasts, the Gutenberg-Richter magnitude-frequency relationship) and a likelihood function, which takes into account observations from the ongoing earthquake. Prior information can be considered relatively static over the timescale of a given earthquake rupture. The changes in the source estimates and predicted peak ground motion distribution, which are updated each second, are due to changes in the likelihood function as additional arrival and amplitude data become available. The potential use of prior information differentiates the VS approach from other regional, network-based EEW algorithms, such as ElarmS (Allen and Kanamori 2003).

Implementation of the VS algorithm in California is an ongoing effort of the Swiss Seismological Service (SED) at ETH Zurich. We prioritized the development of codes involved in real-time data processing, which corresponds to the likelihood function in our Bayesian framework; code development to implement the contribution of prior information is to follow. The VS algorithm is one of three early warning algorithms being implemented and tested in real time as part of the California Integrated Seismic Network (CISN) early warning project; the other two are the ElarmS algorithm of Allen and Kanamori (2003) and the onsite algorithm of Wu and Kanamori (2005). These algorithms send reports to the Southern California Earthquake Center (SCEC) early warning testing Web site, which evaluates performance based on the accuracy and time of availability of magnitude, location, and peak ground motion estimates. Real-time testing will allow the scientific community to establish whether EEW systems can deliver reliable, timely information that can be used in post-earthquake, pre-shaking damage mitigation. In this article, we describe the VS likelihood function, its code architecture, and processing flow and summarize its real-time performance in terms of magnitude and location accuracy in southern California from July 2008 through April 2009.

DESCRIPTION OF THE VS LIKELIHOOD FUNCTION

Conceptually, the VS likelihood function is a set of relationships used to map available arrival and ground motion envelope amplitude information from an ongoing earthquake into estimates of earthquake magnitude, location, depth, origin time, and the distribution of peak ground shaking. All earthquake source parameter and ground motion estimates are updated each second, as additional data become available. A short-term/long-term average (STA/LTA) algorithm based on Allen (1978) is used for automatic picking. The *Binder* Earthworm phase associator codes (Dietz 2002) are adopted to estimate location, depth, and origin time based on available picks. Magnitude estimation and ground motion prediction require the following relationships derived by Cua (2005) and Cua and Heaton (2007): 1) a *P-S* discriminant, 2) a single-station magnitude estimate based on ground motion ratios, 3) envelope attenuation relationships, and 4) a multiple-station magnitude and location estimate. These relationships are based on ground motion envelope values, which are defined as the maximum absolute value on a given channel over a one-second window. The functional forms for these relationships are given below.

1. Swiss Seismological Service, ETH Zurich, Switzerland
2. California Institute of Technology, Pasadena, California, U.S.A.

doi: 10.1785/gssrl.80.5.740

P-S Discriminant

$$PS = 0.4\log_{10}(ZA) + 0.55\log_{10}(ZV) - 0.46\log_{10}(HA) - 0.55\log_{10}(HV) \quad (1)$$

if $PS > -0.1$ then P wave, else S wave.

In Equation 1, *ZA, ZV, HA,* and *HV* denote the vertical acceleration, vertical velocity, and root mean square (rms) horizontal acceleration and rms horizontal velocity envelope values, respectively. This relationship quantifies the concept that *P* waves will have larger amplitudes on the vertical channel, while *S* waves will have larger amplitudes on the horizontal channels.

Single-station Magnitude Estimate

$$ZAD = 0.36\log_{10}(ZA) - 0.93\log_{10}(ZD)$$

if P wave

$$M_{ZAD} = -1.63 \cdot ZAD + 8.94, \sigma_{M_{ZAD}} = 0.45 \quad (2)$$

if S wave

$$M_{ZAD} = -1.46 \cdot ZAD + 8.05, \sigma_{M_{ZAD}} = 0.41$$

In Equation 2, *ZAD* is the ground motion ratio between the vertical acceleration (*ZA*) and vertical displacement (*ZD*) envelope values that best correlates with magnitude (Cua 2005; Cua and Heaton 2007). *ZAD* is inversely proportional to the size of the event. It is relatively larger for small, point-source-type events, which are richer in high frequency energy, and smaller for events that require finite rupture characterization, which are richer in lower frequency energy. The single-station magnitude estimate M_{ZAD} can be calculated as soon as two seconds of *P*-wave amplitude data are available following the STA/LTA pick.

Envelope Attenuation Relationships

$$\log_{10}\bar{Y}(M,R) = aM + bR(M) + d\log_{10}R(M) + e$$
$$R(M) = R + C(M) \quad (3)$$
$$C(M) = c1 \cdot \arctan(M - 5) \cdot \exp(c2 \cdot (M - 5))$$

In Equation 3, M denotes magnitude, while R is epicentral distance in km for $M < 5$ events, and closest distance to the fault or Joyner-Boore distance (Boore and Atkinson 2008), when available for $M > 5$ events. There are 24 separate sets of coefficients (*a, b, c*1, *c*2, *d, e*) for maximum *P*- and *S*-wave amplitudes for horizontal and vertical channels of acceleration, velocity, and displacement on rock and soil sites. These envelope attenuation relationships are valid up to 200 km away from events in the magnitude range $2 < M < 8$. They are used in the multiple-station magnitude and location estimation step (next section), as well as for predicting the geographical distribution of peak ground acceleration and velocity given a magnitude and location estimate. Derivation of these extended magnitude relationships is described in Cua and Heaton (2009).

Multiple-station Magnitude and Location Estimate

$$L(M,\text{lat},\text{lon}) = \sum_{i=1}^{\text{stations}} \sum_{j=1}^{P,S} L(M,\text{lat},\text{lon})_{ij}$$

$$L(M,\text{lat},\text{lon}) = \frac{(ZAD_{ij} - \bar{Z}_j(M))^2}{2\sigma^2_{ZAD_i}} + \sum_{k=1}^{4} \frac{(\log_{10} Y_{obs,ijk} - \log_{10} Y_{ijk}(M,\text{lat},\text{lon})^2}{2\sigma^2_{ijk}} \quad (4)$$

$i = 1,\ldots,n$ where n is the number of stations with P detections

$j = P$ wave, S wave

$k = 1,\ldots,4$ (for ZV, HA, HV, HD channels)

$$\bar{Z}(M)_{iP} = -0.62M + 5.50, \ \sigma_{Z(M)_P} = 0.28$$
$$\bar{Z}(M)_{iS} = -0.69M + 5.52, \ \sigma_{Z(M)_S} = 0.25$$

In Equation 4, *ZAD* is as described in Equation 2, $\log_{10}Y_{ijk}$ is as described in Equation 3, and $\log_{10}Y_{obs,ijk}$ are available observed envelope amplitudes on *ZV, HA, HV,* and *HD* channels. The equations for $Z(M)_{iP}$ and $Z(M)_{iS}$ are the inverses of the single-station magnitude relationships M_{ZAD} in Equation 2.

The magnitude and location coordinates that minimize Equation 4 correspond to the most probable magnitude (*Mvs*) and location estimates given the available observed envelope values. The location estimate corresponds to a strong motion centroid, which is the location of a point source event that best fits the distribution of ground motion amplitudes given a magnitude estimate and a particular attenuation relationship (Kanamori 1993). This centroid location estimate is extremely robust when constrained by a large number of observations but not very stable or precise when using data from only a few stations. Instead, we use the *Binder* location estimate (Dietz 2002), which then reduces the determination of *Mvs* to a 1-dimensional search over magnitude space in Equation 4.

The reader is referred to Cua (2005), Cua and Heaton (2007), and Cua and Heaton (2009) for details on the derivation of these various relationships.

The offline performance of the full Bayesian VS approach (including contributions from both the likelihood function and the prior term) on waveform datasets recorded by the SCSN from the 1999 **M** 7.3 Hector Mine, 2002 **M** 4.8 Yorba Linda, 2003 **M** 6.5 San Simeon, and 2004 **M** 6.0 Parkfield earthquakes is discussed in detail in Cua (2005) and Cua and Heaton (2007).

SYSTEM ARCHITECTURE

Hauksson *et al.* (2006) developed a real-time processing environment that provides an interface between the real-time network data streams and the EEW algorithms participating in the CISN project. What we refer to collectively as the VS codes are the three subsystems (or collections of modules) shown in

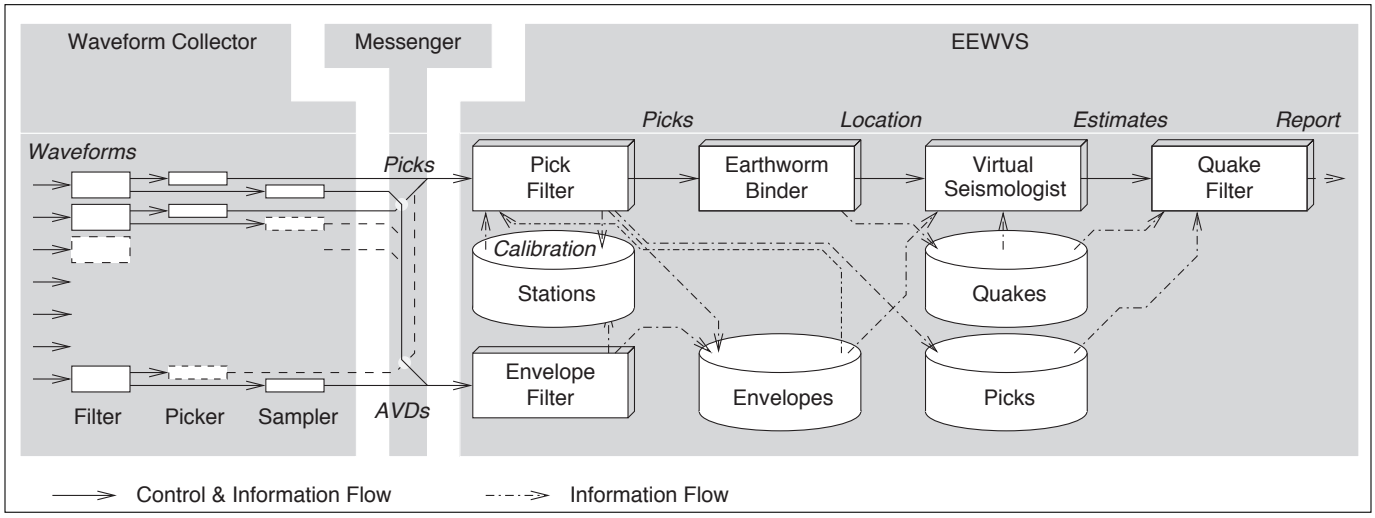

▲ **Figure 1.** System architecture of the VS early warning algorithm. Rectangles represent processing modules, while drums represent dynamic data areas.

Figure 1. Each subsystem has a particular task. The *Waveform Collector* subsystem performs basic waveform processing such as picking, gain correction, baseline removal, filtering, and down-sampling. The ground motion envelope amplitudes of acceleration, velocity, and filtered displacement (AVDs in Figure 1) required as inputs to the VS likelihood function (Cua and Heaton 2007) are calculated here. The *Messenger* subsystem sends information from the *Waveform Collector* subsystem to the *EEWVS* (which stands for Earthquake Early Warning Virtual Seismologist) subsystem. The *EEWVS* subsystem 1) filters and weighs incoming picks, 2) estimates location and origin time based on acceptable picks using the Earthworm *Binder* phase associator, 3) estimates magnitude given the *Binder* location estimate and the available envelope amplitudes using the VS likelihood function relationships, 4) evaluates the reliability of the magnitude and location estimate, and 5) logs the estimated magnitude, location, and predicted peak ground shaking to an event summary file. All event summary files are stored locally for subsequent performance analysis. Event summary files within initial magnitude estimates larger than **M** 2.7 are automatically sent to the SCEC early warning testing Web site. In an operational early warning system, step 5 would include pushing the EEW information to users.

DEALING WITH NOISE IN REAL TIME

To maximize the available warning time, real-time early warning algorithms must decide whether the available data is from an earthquake or noise as early as possible. The following auxiliary algorithms were developed or adopted to assist in this task: 1) pick and envelope filtering, 2) the *Binder* Earthworm phase associator codes (Dietz 2002), and 3) event filtering.

Pick and Envelope Filtering

The VS installation at the SCSN sees real-time data from 170 broadband and strong motion stations; automatic STA/LTA pickers (Allen 1978) report an average of 50,000 picks each day. Ninety percent of these picks are unrelated to earthquake activity. The *Binder* associator (Dietz 2002) can determine whether a given pick can be associated with an earthquake hypocenter or is due to noise, but only when a large number of picks are available. In the interest of minimizing the number of false alarms, we assign quality factors to the incoming picks based on the signal-to-noise ratio. This section describes some empirically determined criteria we have developed for assigning pick quality to picks coming from a standard STA/LTA (Allen 1978) picker algorithm. In the VS codes, an event is declared once four valid (with sufficient quality) picks are available.

The first set of requirements for a pick to be valid are: 1) the maximum velocity on the vertical channel exceeds 0.0001 cm/s (which is the maximum vertical *P*-wave velocity expected from an **M** 3.0 event 50 km away using the Cua and Heaton (2009) envelope attenuation relationships), and 2) the average velocity envelope amplitude three seconds after the pick time exceeds the average velocity envelope amplitude before the pick time. About 80% of raw picks are rejected by these criteria and not used in location estimation; the rejected picks play a later role in distinguishing between correct and incorrect event declarations.

Picks meeting the above requirements are valid picks and are given further quality assignments based on *qv*, the maximum velocity within three seconds of the pick time divided by the average background velocity (essentially the signal-to-noise ratio), and *rp*, the hourly rate of raw picks reported by the STA/LTA picker at the given station. Picks accepted by the trigger discriminant function in Figure 2A are considered triggering picks. At least one triggering pick and three valid picks are required for the initial event declaration. Once an event is declared, location, magnitude, and peak ground motion estimation is initiated by the *EEWVS* subsystem.

The average background velocity is calculated on the vertical velocity channel. We limit the maximum allowable value

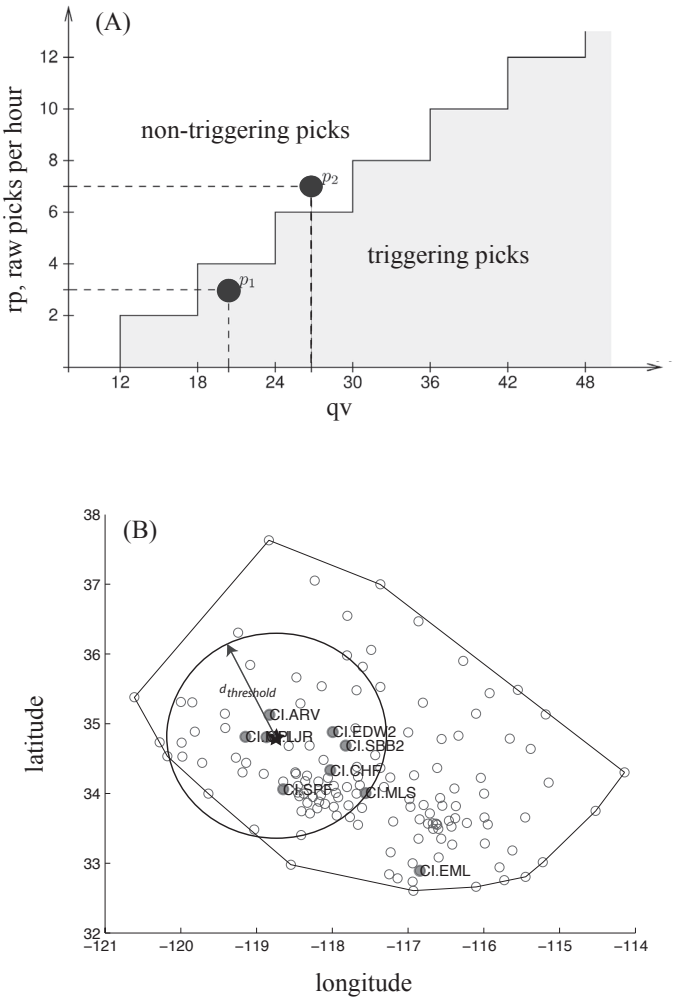

▲ **Figure 2.** (A) The trigger discriminant function as a function of signal-to-noise ratio (qv) and the rate of raw picks. Only triggering picks are allowed to contribute to the initial event declaration. (B) Early warning algorithms must be able to distinguish between local and teleseismic events. The event filter correctly rejects the *Binder* location (star) for the **M** 7.7 Sea of Okhotsk since there are more unpicked stations (open circles) than picked stations (filled circles) within $d_{threshold}$.

of average background velocity to 0.0005 cm/s; without this empirically determined limit, the signal-to-noise ratio is a poor indicator for pick quality during the aftershock sequences of large events. Broadband channels reporting velocities larger than 0.8 cm/s (approximately 80% of the clip level for an STS2) are considered clipped, and subsequent amplitude data from the broadband channels of that station are not used. At stations with both broadband and strong motion instruments, the system switches to using the strong-motion waveforms when the broadband instrument clips.

Binder Earthworm Phase Associator

The *Binder* module is the phase associator used by the Earthworm network processing system (http://www.isti2.com/ew/). Given a set of *P*-wave arrival times, station locations, and a 1-D velocity model, it determines the smallest set of hypocenters consistent with the available picks (Dietz 2002). We configured the *Binder* module to run as soon as at least one triggering pick and three valid picks are available (see section Pick and Envelope Filtering). The location (latitude, longitude, depth, and origin time) estimated by *Binder*'s Simple Event Locator (Dietz 2002) is passed to the Virtual Seismologist module (Figure 1). The Virtual Seismologist module uses the *Binder* location and the available envelope amplitudes to estimate magnitude and the distribution of peak ground acceleration and velocity (currently without site conditions).

Event Filtering

The reliability of the *Binder* location estimate increases with the number of available picks. The initial location estimates can have potentially large errors, since it is possible that one or more of the input picks is from a non-earthquake source. The event filtering module checks whether the magnitude and location estimates are consistent with the available envelope amplitudes and picks. The goal of event filtering is to determine whether a VS event declaration corresponds to a real earthquake (which will eventually have a corresponding entry in the network earthquake catalog) or constitutes a "phantom" event due to random noise-related picks meeting the triggering criteria (which will not match any local earthquake in the catalog but may have an origin time that coincides with a teleseismic event recorded by the network). An EEW algorithm should attempt to maximize its number of real event detections while minimizing the number of phantom event declarations. (Naturally, an EEW algorithm should also attempt to maximize the available warning time by minimizing the time between the earthquake origin time and when the EEW information is available.)

The single-station magnitude estimates M_{ZAD} described in Equation 2 are useful in distinguishing between real and phantom events. We calculate the linear average of the most current single-station magnitude estimates $M_{ZAD,ave}$ available from stations with valid picks. At stations close to the epicenter, the most current single-station magnitude estimate may be based on the *S*-wave envelope amplitudes; at farther stations, these are based on *P*-wave envelope amplitudes. As discussed in the previous section, M_{VS} is the most probable magnitude estimate given the *Binder* location and the available envelope amplitudes. We empirically determined that phantom events typically have $|M_{ZAD,\mathrm{ave}} - M_{VS}| > 1.5$; this criterion can help distinguish between local and teleseismic events.

For real earthquake sources (as opposed to phantom events), we expect that picks will be available at most stations with epicentral distances less than the farthest picked station. Transmission delay or data latency due to different combinations of the type of datalogger and communication link (*i.e.*, radio link, internet, or satellite) between the station and the central processing site ranges between 3 to 13 seconds (with a mean of 6.5 seconds) at the SCSN (Allen 2008). To make allowances for stations with low quality picks and the variation in telemetry delays across different stations, we set the criterion that at least half the stations with epicentral distance less than

$d_{\text{threshold}}$ must report picks (regardless of pick quality) for the event to be valid. In Equation 5,

$$d_{\text{threshold}} = \frac{R_{\max} + \bar{R}}{2}, \quad (5)$$

$R_{\max}$ is the epicentral distance of the farthest picked station, and is the average epicentral distance of remaining picked stations.

Illustrating Event Filtering with M 7.7 Sea of Okhotsk (Teleseismic) Event

An **M** 7.7 earthquake in the Sea of Okhotsk that occurred on 2008/07/05 02:12:03 UTC produced triggers on multiple SCSN stations. There were enough picks of sufficient quality to initiate the calculation of a VS trial solution (magnitude, location, and origin time). Figure 2B shows picked (filled circles) and unpicked (open circles) SCSN stations and the *Binder* epicentral location estimate (star) based on the available picks. The large circle encloses the region with epicentral distance less than $d_{\text{threshold}}$. Since less than half of the stations within this region reported picks, the candidate event is correctly flagged as a phantom event.

The average of the most current single-station magnitude estimates, $M_{ZAD,\text{ave}}$, is 5.15; the most probable magnitude given the *Binder* location estimate and the available envelope amplitudes, M_{VS}, is 3.49. Since $M_{ZAD,ave} - M_{\text{VS}} = 1.66$, the event is declared invalid. *Binder* allows for multiple candidate hypocenters once enough picks are available. For this teleseismic event, the *Binder* module proposed a total of seven candidate hypocenters in southern California (all based on only a few picks), all of which had and were thus flagged as phantom events and rejected. *Binder* would eventually withdraw these erroneous hypocenters itself, once enough picks were available. However, the $|M_{ZAD,\text{ave}} - M_{VS}| > 1.5$ criteria rejects these trial locations much earlier.

If the trial source parameters and the available observations contradict each other, the event estimates are declared invalid—the event is most likely a phantom event. If the trial source parameters and the observations are consistent with each other, the estimates are considered valid and are updated every second until computation times out when no more new picks are reported within a 10-second window.

RESULTS AND DISCUSSION

The VS codes described above have been running in real time at the SCSN since 13 July 2008. Figure 3A shows the real-time SCSN stations, real-time VS event detections (with magnitudes **M** > 1.0), and **M** ≥ 3.0 events missed by the VS codes between 13 July 2008 and 9 April 2009. In generating the performance statistics discussed in this section, we use events listed in the SCSN earthquake catalog within the rectangular region bounded by 31.5 and 37.5 latitude and –121.25 and –114 longitude, since the codes are only installed in southern California. Of the 1,220 reports generated by the VS algorithm over this time period, 1,201 events (98.4%) had estimated origin times within ± 30 seconds of an origin time listed in the SCSN catalog; only 19 (1.6%) were "phantom events" that did not match any local event in the catalog. The VS codes missed 60 out of 107 **M** ≥ 3.0 SCSN events over this time period; the majority of these events are either on the outskirts or outside the network, offshore, or in areas of low station density. Events that occurred while the codes were offline (such as the 28 July 2008 **M** 5.4 Chino Hills earthquake) are also included in the missed event count. The number of valid missed **M** ≥ 3.0 events (or events that the codes should have detected but did not, for reasons yet unresolved) is on the order of 10 events. The evolution of VS magnitude and location estimates as a function of time for the **M** 5.4 28 July 2008 Chino Hills event and the **M** 5.1 5 December 2008 event near Barstow, California (which were the two largest events that occurred during the period covered by this study) are shown in Figures 3B through 3E.

Figure 4A shows a histogram of when the initial VS estimates are available relative to the earthquake origin time. Eighty-two percent and 96.5% of events detected by the VS codes have initial estimate times within 25 and 30 seconds of the origin time, respectively. The mean time to the initial VS estimate is 21.9 seconds. These initial estimate times are dominated by the time for four acceptable picks to be available; the effects of telemetry delay—SCSN stations have a median telemetry delay of 6.5 seconds (Allen 2008)—and processing time (~3 seconds) are also included. Figure 4B shows contours of approximate initial VS estimate time (time for *P* waves to propagate to four stations + 6.5 seconds average telemetry delay + 3 seconds processing time) in southern California given the locations of current SCSN stations. More aggressive use of prior information can potentially decrease the initial estimate time and thus increase the available warning time for potential users. In particular, the method of Voronoi cells and not-yet-arrived data can potentially provide location estimates as early as the first *P* wave is detected (Cua 2005; Cua and Heaton 2007; Horiuchi *et al.* 2005; Satriano *et al.* 2007). However, such approaches need significant modification to work with networks such as SCSN with non-uniform station telemetry delays.

The *Binder* module gives stable location estimates if noise-related picks are properly filtered out by pick filtering and not included in the initial event declaration. The median error of the initial epicentral location estimate for the 1,201 detected events is 2.6 km. Magnitude estimation performance is shown in Figure 5. The CISN early warning project aims to evaluate early warning algorithm performance for **M** ≥ *3.0* events. There have not been many **M** ≥ *3.0* events since the codes started operating; 1,094 out of 1,201 (91%) of the VS detected events are in the microearthquake range with magnitudes **M** < 3.0. The VS algorithm is based on envelope attenuation relationships derived from a dataset spanning the magnitude range 2.0 < **M** ≤ 7.5 (Cua and Heaton 2008). It can thus operate at **M** < 3.0 level, with some systematic overestimation expected due to the vicinity of the operating range to the lower magnitude limit of the attenuation relationships (Bommer *et al.* 2007). Given a reasonable location estimate (94% of events have initial location estimates within 20 km of the actual epicenter),

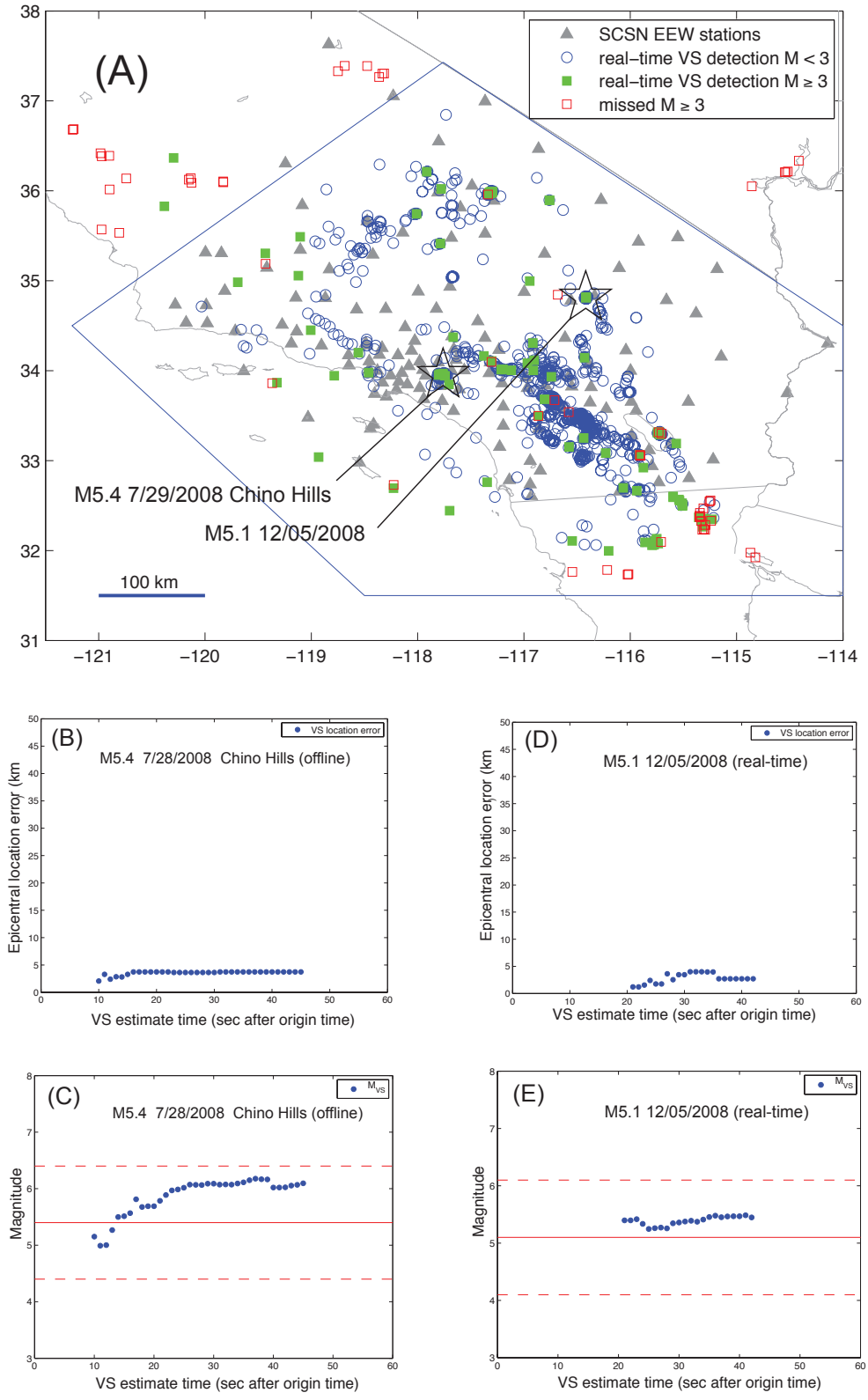

▲ **Figure 3.** (A) VS real-time performance in southern California during 13 July 2008–9 April 2009. The polygon encloses the SCSN area of responsibility (AOR). (B and C) Evolution of VS epicentral location and magnitude error, respectively, as a function of time for the **M** 5.4 28 July 2008 Chino Hills earthquake. The VS codes were offline at the time of the event due to a scheduled code upgrade. Results shown were generated using a waveform dataset for the Chino Hills event downloaded from the Southern California Earthquake Data Center (SCECDC). (D and E) Evolution of VS epicentral location and magnitude error, respectively, as a function of time for an **M** 5.1 5 December 2008 earthquake near Barstow, California. Results shown were generated in real time.

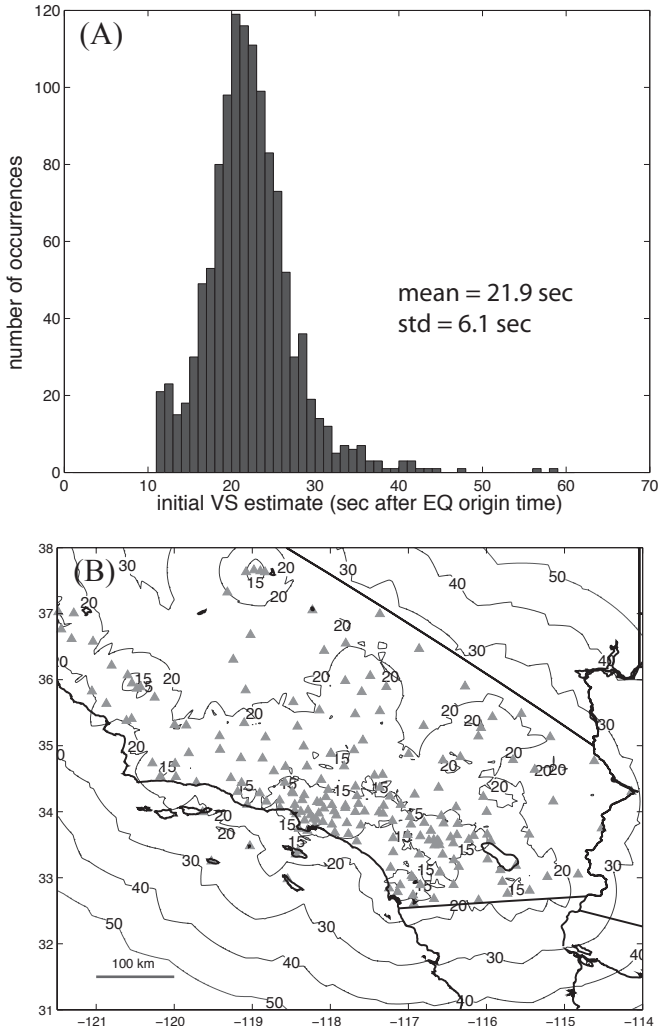

▲ **Figure 4.** (A) Histogram of the initial VS estimate time. Eighty-two percent of events have initial estimates available within 25 seconds of event origin time. Events with initial estimate times larger than 30 seconds are typically events on the outskirts or outside the network. (B) Contours of approximate initial VS estimate time in southern California given the current SCSN station configuration (gray triangles).

the error of the initial magnitude estimate has a median of 0.17. The current version of the VS codes does not take site conditions into account; thus, ground motion amplification effects are always mapped into larger magnitude estimates. Magnitude estimates, which are updated each second, typically increase with time as the ground motions propagate to the concentration of stations in the Los Angeles basin, which experiences significant site amplification. Table 1 summarizes the M_{VS} error statistics at various magnitude ranges. Site conditions will be taken into account in future versions of the VS codes.

CONCLUSIONS

The Virtual Seismologist codes have been running in real time at the SCSN since July 2008. The auxiliary methods we developed or adopted to assist in noise discrimination—pick and envelope filtering, the *Binder* associator, and event filtering—work reasonably well in southern California. All VS event detections that had corresponding entries in the SCSN catalog (thus excluding phantom events) during the time period covered by this study have initial magnitude estimates that would be considered correct, based on the SCEC acceptance criteria of ±1 magnitude unit of error relative to the network magnitude. The noise-related issues have a significant impact on VS performance due to the decision to allow the codes to trigger on microearthquakes with magnitude below 3.0; 90% of the events declared by the VS codes fall within this category. While it can be argued that evaluating the performance of an EEW algorithm at the microearthquake level is irrelevant (since EEW is most useful for larger earthquakes that can cause damage), mistakenly identifying a microearthquake as a damaging earthquake would undermine the credibility of an operational EEW system. Operating the VS codes at the microearthquake level allows us to determine the possible sources of such errors and test the codes frequently. The performance of the VS codes in terms of magnitude and location estimation shows its promise as an EEW algorithm. However, an operational EEW system will require improvements in how fast EEW information can be made available to potential users. Our subsequent efforts will be focused on exploiting relevant prior information (whose inclusion in the source estimation process is facilitated by the Bayesian VS framework), in particular network geometry and the concept of not-yet-arrived data, to reduce the time to the initial estimate and thus increase the available warning time.

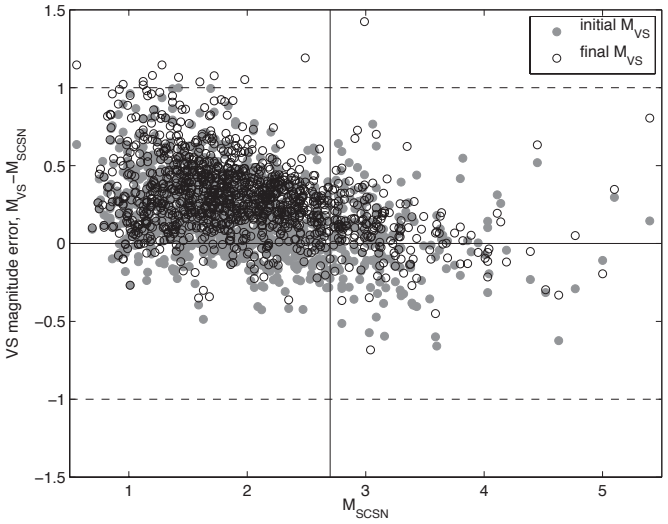

▲ **Figure 5.** VS magnitude error as a function of the network magnitude, M_{SCSN}. The systematic overestimation of M_{VS} at the **M** < 3.0 range is in part due to using the Cua and Heaton (2009) envelope attenuation relationships in the vicinity of their lower magnitude limit of **M** 2.0 and in part to uncorrected site amplification effects.

TABLE 1
Statistics of initial and final M_{VS} relative to the network magnitude (M_{SCSN}) for various magnitude ranges

Magnitude Range	% of Total Events	Initial $M_{VS} - M_{SCSN}$ (in magnitude units)	Final $M_{VS} - M_{SCSN}$ (in magnitude units)
1.0 < **M** < 3.0	91% (1,097 out of 1,201)	mean = 0.19 std = 0.23	mean = 0.3 std = 0.23
M ≥ 3.0	9% (107 out of 1,201)	mean = –0.03 std = 0.27	mean = 0.05 std = 0.22
Entire range	100%	mean = 0.17 std = 0.25	mean = 0.29 std = 0.24

ACKNOWLEDGEMENTS

This work was supported by EC-FP6-Project SAFER contract 036935 and EC-Project NERIES contract 026130. The Southern California Seismic Network (SCSN) and the Southern California Earthquake Data Center (SCEDC) are funded through contracts with USGS/ANSS, the California Office of Emergency Services (OES), and the Southern California Earthquake Center (SCEC).

REFERENCES

Allen, R. (2008). *CISN Earthquake Early Warning: Testing of Seismological Algorithms*. Internal report, submitted to U.S. Geological Survey.

Allen, R. M., and H. Kanamori (2003). The potential for earthquake early warning in southern California. *Science* **300** (5620), 786–789.

Allen, R. V. (1978). Automatic earthquake recognition and timing from single traces. *Bulletin of the Seismological Society of America* **68** (5), 1,521–1,532.

Bommer, J. J., P. J. Stafford, J. E. Alarcon, and S. Akkar (2007). The influence of magnitude range on empirical ground-motion prediction. *Bulletin of the Seismological Society of America* **97** (6), 2,152–2,170.

Boore, D. M., and G. M. Atkinson (2008). Ground motion prediction equations for the average horizontal component of PGA, PGV, and 5%-damped PSA at spectral periods between 0.01 s and 10.0 s. *Earthquake Spectra* **24**, 99–138.

Cua, G. (2005). *Creating the Virtual Seismologist: Developments in Ground Motion Characterization and Seismic Early Warning*. Ph. D. Thesis: California Institute of Technology.

Cua, G., and T. Heaton (2007). The Virtual Seismologist (VS) method: A Bayesian approach to earthquake early warning. In *Earthquake Early Warning Systems*, ed. P. Gasparini, G. Manfredi, and J. Zschau, 97–132. Berlin and Heidelberg: Springer.

Cua, G., and T. Heaton (2009). Characterizing average properties of southern California ground motion amplitudes and envelopes.

Dietz, L. (2002). *Notes on Configuring BINDER_EW: Earthworm's Phase Associator*; http://www.isti2.com/ew/ovr/binder_setup.html.

Hauksson, E., K. Solanki, P. Friberg, D. Given, P. Maechling, D. Neuhauser, and M. Helweg (2006). Implementation of Real-Time Testing of Earthquake Early Warning Algorithms Using the California Integrated Seismic Network Infrastructure as a Test Bed. Abstract, *Seismological Society of America Annual Meeting,* April 2006, San Francisco, California.

Horiuchi, S., H. Negishi, K. Abe, A. Kamimura, and Y. Fujinawa (2005). An automatic processing system for broadcasting earthquake alarms. *Bulletin of the Seismological Society of America* **95** (2), 708–718.

Kanamori, H. (1993). Locating earthquakes with amplitude: Application to real-time seismology. *Bulletin of the Seismological Society of America* **83**, 264–268.

Satriano, C., A. Lomax, and A. Zollo (2007). Optimal, real-time earthquake location for early warning. In *Earthquake Early Warning Systems*, ed. P. Gasparini, G. Manfredi, and J. Zschau, 45–63. Berlin and Heidelberg: Springer.

Wu, Y.-M., and H. Kanamori (2005). Experiment on an onsite early warning method for the Taiwan early warning system. *Bulletin of the Seismological Society of America* **95** (1), 347–353.

Swiss Seismological Service
ETH Zurich
Switzerland
georgia.cua@sed.ethz.ch
(G. C.)